Myosin Surface Loop 4 Modulates Inhibition of Actomyosin 1b ATPase Activity by Tropomyosin†

Alena Lieto-Trivedi, Sheffali Dash, and Lynne M. Coluccio*

Boston Biomedical Research Institute, 64 Grove Street, Watertown, Massachusetts 02472

Received November 27, 2006; Revised Manuscript Received January 4, 2007

ABSTRACT: Structural studies of the class I myosin, MyoE, led to the predictions that loop 4, a surface loop near the actin-binding region that is longer in class I myosins than in other myosin subclasses, might limit binding of myosins I to actin when actin-binding proteins, like tropomyosin, are present, and might account for the exclusion of myosin I from stress fibers. To test these hypotheses, mutant molecules of the related mammalian class I myosin, Myo1b, in which loop 4 was truncated (from an amino acid sequence of RMNGLDES to NGLD) or replaced with the shorter and distinct loop 4 found in *Dictyostelium* myosin II (GAGEGA), were expressed in vitro and their interaction with actin and with actin-tropomyosin was tested. Saturating amounts of expressed fibroblast tropomyosin-2 resulted in a decrease in the maximum actin-activated Mg^{2+}-ATPase activity of wild-type Myo1b but had little or no effect on the actin-activated Mg^{2+}-ATPase activity of the two mutants. In motility assays, few actin filaments bound tightly to Myo1b-WT-coated cover slips when tropomyosin-2 was present, whereas actin filaments both bound and were translocated by Myo1b-NGLD or Myo1b-GAGEGA in both the presence and absence of tropomyosin-2. When expressed in mammalian cells, like the wild type, the mutant myosins were largely excluded from tropomyosin-containing actin filaments, indicating that in the cell additional factors besides loop 4 determine targeting of myosins I to specific subpopulations of actin filaments.

How myosin motors, of which there are possibly 25 classes, many with multiple isoforms (*1*−*3*), are directed to specific sites in the cell is an important question in cell biology. Previous studies have shown that epitope-tagged mammalian class I myosin, Myo1b, associates with dynamic actin structures in the cell but is excluded from the more stable tropomyosin-2-containing stress fibers (*4*). Tropomyosin-2 (Tm-2),[1] a high-molecular weight α-tropomyosin gene product, is one of seven tropomyosin isoforms found in rat fibroblasts, where it is present in major abundance. In cultured epithelial cells, Tm-2 is found to be associated with basolateral membranes (*5*). Tropomyosins bind along the length of actin filaments and contribute to the stability of actin filaments by guarding against depolymerization (*6*), fragmentation (*7*, *8*), and branching (*9*). Much of what is known regarding binding of tropomyosin to actin comes from studies with skeletal muscle proteins. The prevailing theory is that tropomyosin strands lay in the long pitch grooves of F-actin and move upon activation, leaving the actin exposed for interaction with myosin (*10*).

The actin-binding region of myosin consists of a number of regions, including the helix−loop−helix motif of the lower 50 kDa domain, loop 2, the cardiomyopathy loop, loop 3, and loop 4 (*11*, *12*). The helix−loop−helix motif defining the primary actin-binding site is consistent among myosins, but the polar and charged loops of the upper 50 kDa domain and the secondary actin-binding sites, which act as modulators of actin binding, vary in length, sequence, and conformation (*12*). Specific structural elements present in the Myo1b motor domain might prevent Myo1b from associating with tropomyosin-containing microfilaments, but which element(s) is unknown.

Insight comes from examination of the crystal structure of *Dictyostelium discoideum* MyoE (*12*), which is in the same myosin I subclass as mammalian Myo1b, the focus of this study (*1*) (Figure 1). The MyoE structure shows that loop 4, which contains many charged amino acid residues and is longer in *Dictyostelium* MyoE and mammalian Myo1b by four to five residues versus other myosins, extends from the surface in the vicinity of the actin-binding region, suggesting that loop 4 might interfere with binding of class I myosins to actin when regulatory proteins are present (*12*). Loop 4 is termed the cardiac or C-loop in β-cardiac muscle myosin II (*13*). Molecular modeling of chicken skeletal muscle myosin II and F-actin places the cardiac loop near the cardiomyopathy loop at the actin-binding face (*11*, *14*), where it interacts with lysine 328 of actin (*15*). Proteolytic cleavage of the C-loop in β-cardiac muscle myosin II eliminates the actin-activated myosin ATPase activity and substantially reduces the affinity of myosin II for actin (*16*). Studies with smooth muscle myosin II have shown that the charge of the C-loop is important in determining the affinity of that myosin for actin, its maximum ATPase activity, and in vitro motility (*16*).

† This work was supported by NIH Grant R01 GM68060 to L.M.C. A.L.-T. is the recipient of a Ruth L. Kirschstein National Research Service Award (GM072332).

* To whom correspondence should be addressed: Boston Biomedical Research Institute, 64 Grove St., Watertown, MA 02472. Telephone: (617) 658-7784. Fax: (617) 972-1761. E-mail: coluccio@bbri.org.

[1] Tm-2, tropomyosin-2.

10.1021/bi602439f CCC: $37.00
Published on Web 02/14/2007

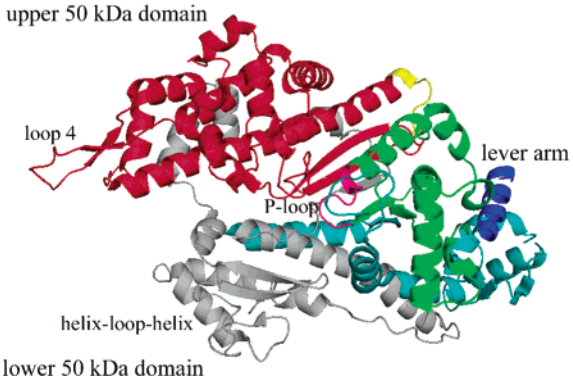

FIGURE 1: Cartoon produced with the molecular visualization program MacPyMol (http://www.pymol.org) of the motor domain of the MyoE structure from *D. discoideum* determined by Kollmar and colleagues (*12*): N-terminus, green; upper 50 kDa domain, red; lower 50 kDa domain, gray; P-loop, magenta; converter region, teal; and lever arm, blue. The actin-binding region includes loop 4, a surface loop in the upper 50 kDa domain, and the helix−loop−helix region, in the lower 50 kDa domain.

To test the hypothesis that loop 4 modulates binding of Myo1b to actin-tropomyosin, mutant Myo1b in which loop 4 was truncated (Myo1b-NGLD) and a chimera in which loop 4 was replaced with the corresponding loop 4 from *Dictyostelium* myosin II (Myo1b-GAGEGA), which is shorter than loop 4 in wild-type Myo1b, were expressed, and the interaction with actin or with actin-tropomyosin was investigated with actin-activated Mg^{2+}-ATPase assays and motility assays and compared to that of the wild type. Then, to test whether modifying loop 4 results in association of Myo1b with stress fibers in cells, wild-type and mutant Myo1b were transiently transfected into HeLa and NRK cells, and their localization was assessed by indirect immunomicroscopy.

We show here that the inhibition of motor activity of Myo1b observed in the presence of tropomyosins is removed when loop 4 is truncated or replaced with a corresponding loop 4 from another myosin; however, these modifications of loop 4 do not result in colocalization of Myo1b with tropomyosin-containing microfilaments in the cell. We propose that loop 4 modulates the interaction of Myo1b with actin-tropomyosin but is not sufficient to dictate how class I myosins are targeted to specific populations of actin filaments in the cell.

EXPERIMENTAL PROCEDURES

Preparation of Actin and Tropomyosin. Actin was prepared from rabbit skeletal muscle according to the procedure of Spudich and Watt (*17*) and further purified by column chromatography (*18*). Actin was stored in filamentous form at −80 °C until it was used. Tm-2 was prepared as previously described (*19*) and stored in solution at −80 °C. Protein concentrations were determined with the Bio-Rad protein assay (Bio-Rad Laboratories, Inc., Hercules, CA).

Construction of Loop 4 Mutants and Expression in Insect and Mammalian Cells. The amino acid sequences of the loop 4 region for skeletal muscle myosin II (Sk), *Dictyostelium* myosin II (Dy), smooth muscle myosin II (Sm), Myo1b, and *Dictyostelium* MyoE were aligned using Clustal X (http://searchlauncher.bcm.tmc.edu/multi-align/multi-align.html) and shaded to show conservation using Boxshade (http://www.ch.embnet.org/software/BOX_form.html) (Figure 2). The secondary structure assignments noted above the Sk sequence were made with DSSP[2] (*20*) for the high-resolution structure of *Dictyostelium* myosin II[3] (1VOM) (*21*). The secondary structure assignments noted below the MyoE sequence are for MyoE[4] (*12*).

Constructs were designed to avoid disruption of the secondary structure of the two α-helices that are amino- and carboxyl-terminal to loop 4. Wild-type (WT) loop 4 (RMNGLDES) was replaced with a truncated version of the original loop containing amino acids NGLD (NGLD) or the shorter loop from *Dictyostelium* myosin II (GAGEGA) (see Table 1 for a list of constructs used and their descriptions). To define the beginning and end of loop 4 in various myosins, secondary structure assignments were made with DSSP (*20*) using the structures of *Dictyostelium* myosin II (*21*) and MyoE (*12*) as guides. Two unique restriction sites flanking loop 4 were introduced through silent mutation, and then an in-frame fusion protein was created by polymerase chain reaction. Mutants were made by enzymatically digesting the vector at the unique restriction sites and then ligating in the duplex DNA representing the different mutations. Full-length (Myo1b) myc- and FLAG-tagged mutants were made as well as FLAG-tagged truncated forms ($Myo1b^{1IQ}$) representing the motor domain and the first IQ domain of Myo1b (amino acids 1−728). This S1-like construct displays steady- and transient-state kinetics indistinguishable from those of the parent molecule (*22*, *23*). In each case, expression of the truncated mutant was at a higher level than the corresponding full-length constructs, so the 1IQ forms were used for the ATPase assays to satisfy protein requirements.

After sequences were verified, the constructs were expressed using the Bac-to-Bac Baculovirus Expression System (Invitrogen Life Technologies, Carlsbad, CA) along with calmodulin. After infection for 4 days, the insect cell pellets were homogenized in 10 mM Tris (pH 7.5), 0.2 M NaCl, 4 mM $MgCl_2$, and 2 mM ATP and then centrifuged at 50000*g* for 1 h. The supernatant was applied to an anti-FLAG column, and the expressed protein was eluted with a step gradient of FLAG peptide (*22*). Fractions containing protein were identified by SDS−polyacrylamide gel electrophoresis, pooled, and dialyzed against 10 mM Tris (pH 7.5), 50 mM KCl, and 1.0 mM DTT. Proteins were used immediately or stored at −80 °C for future use. Protein concentrations were determined with the Bio-Rad protein assay. The protein concentration of the fractions eluting from the column and the total yield varied with the preparation.

[2] DSSP, definition of the secondary structure of proteins.

[3] The atomic coordinates for the crystal structure of this protein are available in the Research Collaboratory for Structural Bioinformatics Protein Data Bank as entry 1VOM.

[4] The atomic coordinates for the crystal structure of this protein are available in the Research Collaboratory for Structural Bioinformatics Protein Data Bank as entry 1LKX.

[5] The amino acid sequence of this protein can be accessed through the NCBI Protein Database as NCBI accession number P13538.

[6] The amino acid sequence of this protein can be accessed through the NCBI Protein Database as NCBI accession number P08799.

[7] The amino acid sequence of this protein can be accessed through the NCBI Protein Database as NCBI entry P10587.

[8] The amino acid sequence of this protein can be accessed through GenBank as entry X68199.

[9] The amino acid sequence of this protein can be accessed through the NCBI Protein Database as NCBI accession number Q03479.

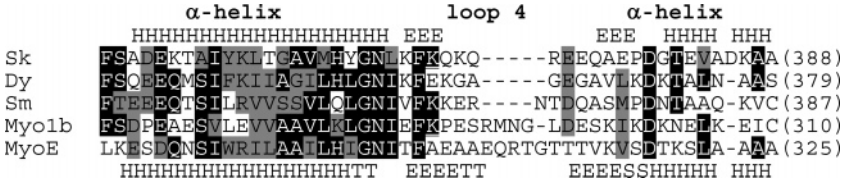

FIGURE 2: Alignment by Clustal X and shading by Boxshade of loop 4 regions from skeletal muscle myosin II[5] (Sk), *Dictyostelium* myosin II[6] (Dy), smooth muscle myosin II[7] (Sm), myosin 1b[8] (Myo1b), and myosin E[9] (MyoE). See the text for how secondary structure assignments were made. Abbreviations: H, α-helical region; E, extended strand that participates in the β-ladder; T, hydrogen-bonded turn; S, bend.

Table 1: Constructs Used in This Work

Myo1b-WT	full-length wild-type Myo1b; loop 4 sequence, RMNGLDES
Myo1b-NGLD	Myo1b in which wild-type loop 4 is truncated to NGLD
Myo1b-GAGEGA	Myo1b in which wild-type loop 4 is replaced with loop 4 of *Dictyostelium* myosin II, GAGEGA
Myo1b^{1IQ}-WT	wild-type Myo1b truncated after the first IQ domain at amino acid 728 containing the wild-type loop 4 sequence, RMNGLDES
Myo1b^{1IQ}-NGLD	Myo1b^{1IQ} in which wild-type loop 4 is truncated to NGLD
Myo1b^{1IQ}-GAGEGA	Myo1b^{1IQ} in which wild-type loop 4 is replaced with loop 4 of *Dictyostelium* myosin II, GAGEGA

Efforts to concentrate the samples with centrifugal filtration devices were unsuccessful as they resulted in a loss of activity.

For expression in mammalian cells, full-length wild-type and mutant Myo1b were cloned into pCMV-myc (CLONTECH Laboratories, Palo Alto, CA), which expresses proteins containing the N-terminal c-Myc epitope tag. Myo1b was also expressed as a fusion protein with enhanced green fluorescent protein at the C-terminus by cloning the Myo1b gene into plasmid pEGFP-N1 (CLONTECH Laboratories).

Actin-Activated Mg^{2+}-ATPase Activity. The actin-activated Mg^{2+}-ATPase activity was evaluated at 37 °C in 10 mM Tris (pH 7.5), 50 mM KCl, 1 mM DTT, 1 mM $MgCl_2$, 1 mM ATP, and the appropriate ratio of 2 mM EGTA to 2 mM CaEGTA to effect pCa values of 4.6 or 8.9 (*24*, *25*) using a colorimetric assay that measures phosphate (*26*). Standard curves were generated with known amounts of phosphate. To determine K_m and V_{max}, the data were fit to hyperbolae using Origin 7 (Microcal, Northampton, MA).

Actin Binding Assay. The interaction of Myo1b^{1IQ} and the loop 4 mutants with filamentous rabbit skeletal muscle actin with or without Tm-2 was investigated using cosedimentation assays as previously described (*27*). Briefly, 6 μM actin and 2.5 μM Tm-2 were incubated for 30 min before addition of either ~7 μg of Myo1b^{1IQ} or ~7 μg of the loop 4 mutants. After an additional 30 min, the samples were centrifuged at 100000*g* for 20 min. Supernatants were removed and precipitated with 10% trichloroacetic acid. The precipitated proteins were collected in a microfuge tube, then solubilized in 1 M Tris base, and prepared for sodium dodecyl sulfate−polyacrylamide gel electrophoresis (SDS−PAGE) (*28*). Pellets were solubilized directly in 1 M Tris base and then prepared for SDS−PAGE. Samples were electrophoresed on 7.5/15% acrylamide split mini-gels (*27*). The relative amounts of Myo1b^{1IQ} or the loop 4 mutants in the pellets were determined by NIH Image (version 1.61; http://rsb.info.nih.gov/nih-image).

Motility Assays. The ability of full-length Myo1b and the loop 4 mutants to translocate actin filaments was determined in vitro in the presence and absence of Tm-2 using the sliding filament assay adapted from that of Toyoshima et al. (*29*). Cover slips were coated with 0.1% nitrocellulose in amyl acetate and flow chambers were constructed by attaching the nitrocellulose-coated cover slips face down to a glass slide using double-sided sticky tape. Ten microliters of the myosin solution at ~50 μg/mL was infused and incubated for 15 min. This step was repeated if the myosin concentration was low. The sample chambers were then washed with 75 μL of 5 mg/mL bovine serum albumin (BSA) in buffer M [25 mM imidazole (pH 7.4), 1 mM EGTA, 25 mM KCl, 4 mM $MgCl_2$, and 1 mM DTT], and incubated for 5 min. Thirty microliters of 0.13 μM rabbit skeletal muscle F-actin labeled with rhodamine phalloidin (prepared as suggested by Molecular Probes, Eugene, OR) with or without 2.3 μM Tm-2 was applied to the sample chamber and allowed to bind for 5 min. As a control, association of Tm-2 with actin under the defined conditions of the motility assays was verified in cosedimentation assays (data not shown). The chamber was washed with 75 μL of buffer M containing 5 mg/mL BSA prior to the initiation of motility with the addition of buffer M with 2 mM ATP, 0.5% methylcellulose, 20 mM DTT, 3 mg/mL glucose, 0.1 mg/mL glucose oxidase, and 0.02 mg/mL catalase (*30*). Slides were examined with a Nikon fluorescence microscope using a 100× oil immersion lens (Nikon Inc., Melville, NY). Images were recorded digitally using a FlashBus MV PCI bus frame grabber (Integral Technologies, Inc., Indianapolis, IN). The speed of the filaments was determined using the Track Points application in MetaMorph bioimaging software (version 6.3r2, Universal Imaging Corp., Downingtown, PA). Data are presented as average speeds ± the standard deviation (number of filaments).

Cellular Localization of Myo1b and Loop 4 Mutants. HeLa (cervical cancer epithelial cells) and NRK (normal rat kidney) cells were transfected 1 day after plating or in suspension with FuGENE 6 Transfection Reagent (Roche Applied Science, Indianapolis, IN) and vectors representing the full-length Myo1b-WT-pCMV-myc, or mutants, Myo1b-NGLD-pCMV-myc or Myo1b-GAGEGA-pCMV-myc, and then grown on glass cover slips. After 3−48 h depending on the experiment, the cells were fixed in formaldehyde and Myo1b was localized by indirect immunofluorescence microscopy with mouse monoclonal 9E10 anti-myc followed by detection with Alexa^{488}-labeled goat anti-mouse IgG or with rabbit polyclonal anti-myc (Cell Signaling Technology, Inc., Beverly, MA) followed by Alexa^{488}-labeled goat anti-rabbit IgG. As a control, some cells were transfected with enhanced green fluorescent protein-tagged non-muscle myosin II-B

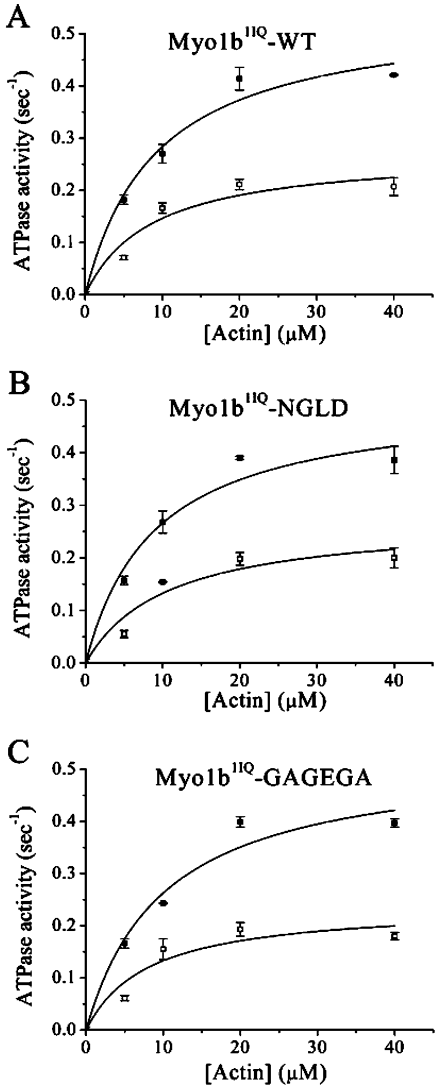

FIGURE 3: ATPase activity of Myo1b^{1IQ}-WT and loop 4 mutants. Actin-activated Mg^{2+}-ATPase activities were measured at 0−40 μM phalloidin-stabilized actin at pCa 4.6 (■) and 8.9 (□) for 7 μg of Myo1b^{1IQ}-WT (A), Myo1b^{1IQ}-NGLD (B), or Myo1b^{1IQ}-GAGEGA (C). Error bars represent standard deviations of duplicate samples performed at the same time.

[CMV-GFP-NMHC II-B (*31*); Addgene plasmid 11348]. Tropomyosin-containing filaments were identified with mouse monoclonal antibody TM311 (Sigma, St. Louis, MO), which was raised against chicken gizzard tropomyosin but recognizes cytoplasmic tropomyosins from several species, followed by Alexa^{568}-labeled goat anti-mouse IgG. In some cases, the cells were treated with cytoskeleton stabilization buffer containing streptolysin O after fixation (*4*). As an alternative to tropomyosin staining, the cytoskeleton was visualized with rhodamine-labeled phalloidin per manufacturer's instructions (Molecular Probes). Cover slips were viewed with a 60× oil immersion objective on a Bio-Rad Laser Scanning Radiance 2000 confocal microscope (Carl Zeiss MicroImaging, Inc., Thornwood, NY). Images were processed with the associated LaserSharp 2000 software and Adobe Photoshop.

RESULTS

ATPase Activity. As previously observed (*22*), the Mg^{2+}-ATPase activity of a truncated form of Myo1b consisting of the motor domain and first IQ domain, Myo1b^{1IQ}-WT, was activated by actin. Also, as previously shown for class I myosins, which are regulated through Ca^{2+}-bound calmodulin (*32*−*34*), the level of actin activation was higher at pCa 4.6 than at pCa 8.9 (Figure 3A). Little or no difference in K_m and V_{max} was observed for Myo1b^{1IQ} in which loop 4 was shortened (Myo1b^{1IQ}-NGLD) (Figure 3B) or replaced with the shorter loop 4 from *Dictyostelium* myosin II (Myo1b^{1IQ}-GAGEGA) (Figure 3C and Table 2).

At pCa 4.6 in the presence of 8 μM Tm-2, the V_{max} for Myo1b^{1IQ}-WT was reduced by approximately 60%, while the K_m was unaffected (Figure 4A and Table 2). In contrast, Myo1b^{1IQ}-NGLD showed little or no change in either the V_{max} or the K_m in the presence of Tm-2 (Figure 4B). Substitution of the wild-type loop 4 for the analogous loop in *Dictyostelium* myosin II had an intermediate effect with a reduction in V_{max} by 20% (Figure 4C). The results were confirmed with additional sets of experiments performed at 15 and 30 μM actin (data not shown).

Actin Binding Assay. In cosedimentation assays, after a 30 min incubation, the majority of Myo1b^{1IQ} (Figure 5A), Myo1b^{1IQ}-NGLD (Figure 5B), or Myo1b^{1IQ}-GAGEGA (Figure 5C) associated with the actin filaments and was found in the pellet. There was no significant change in the amount of Myo1b^{1IQ} or loop 4 mutants bound to actin in the presence of Tm-2 (Figure 5D). These studies were repeated several times at different protein concentrations with the same result. Moreover, in three separate experiments, no difference in the amount of Myo1b or the loop 4 mutants cosedimenting with actin filaments with or without Tm-2 was observed when the experiments were conducted in the presence of 5 mM ATP (data not shown), indicating that even under conditions in which Myo1b is expected to bind actin weakly, Tm-2 has no effect. In two separate experiments, it was also determined that the amount of Tm-2 associating with actin is not affected by pretreatment of actin with Myo1b^{1IQ} (data not shown).

Motility Assays. Rhodamine-labeled actin filaments bound to full-length Myo1b attached to the surface of a nitrocellulose-coated cover slip, and with the addition of ATP, the actin filaments moved in a directed fashion at a rate of 20 ± 5 nm/s (Myo1b-WT) (Table 3). The number of actin filaments that tightly attached to the wild-type Myo1b substrate was significantly reduced in the presence of Tm-2. The small percentage of actin−Tm-2 filaments that did bind to the surface moved at a rate comparable to control

Table 2: Analysis of Steady-State Actin-Activated Mg^{2+}-ATPase Assays with or without 8 μM Tm-2

	Myo1b^{1IQ}-WT		Myo1b^{1IQ}-NGLD		Myo1b^{1IQ}-GAGEGA	
	V_{max} (s^{-1})	K_m (μM)	V_{max} (s^{-1})	K_m (μM)	V_{max} (s^{-1})	K_m (μM)
pCa 4.6	0.54 ± 0.06	9 ± 3	0.50 ± 0.06	9 ± 3	0.53 ± 0.07	10 ± 4
pCa 8.9	0.27 ± 0.05	9 ± 5	0.27 ± 0.06	11 ± 6	0.24 ± 0.05	8 ± 5
pCa 4.6 with Tm-2	0.21 ± 0.02	11 ± 2	0.53 ± 0.07	13 ± 4	0.42 ± 0.04	9 ± 3

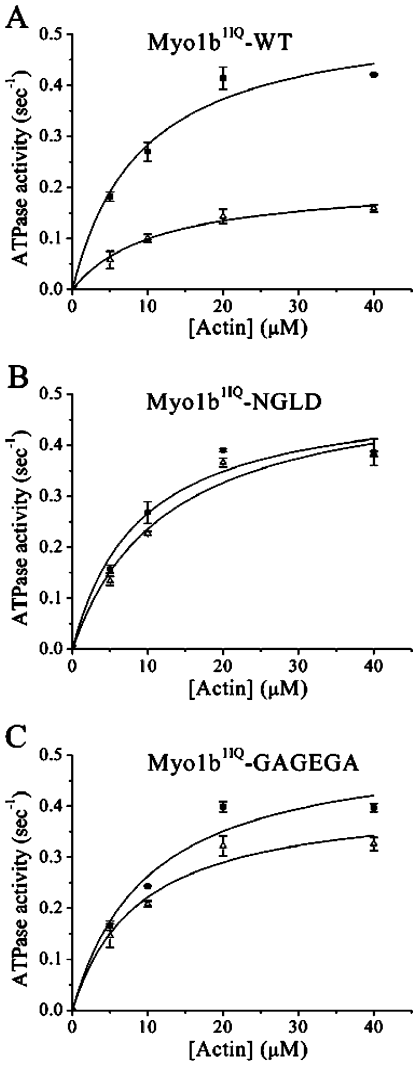

FIGURE 4: ATPase activity of Myo1b^{1IQ}-WT and loop 4 mutants in the presence of Tm-2. Shown are the Mg^{2+}-ATPase activities at 0−40 μM phalloidin-stabilized actin in the absence (■) and presence of saturating amounts (8 μM) of Tm-2 (△) for 7 μg of Myo1b^{1IQ}-WT (A), Myo1b^{1IQ}-NGLD (B), or Myo1b^{1IQ}-GAGEGA (C). The values and error bars represent the averages and standard deviations of duplicates performed at the same time.

values; however, their motion did not appear as smooth and continuous as in the absence of Tm-2. This is consistent with previous studies which showed that Tm-2 inhibits the translocation of actin by Myo1b (*4*).

Myo1b-NGLD also supported the translocation of actin filaments in vitro (34 ± 9 nm/s). In addition, actin−Tm-2 filaments bound to Myo1b-NGLD immobilized on nitrocellulose and were translocated in the presence of ATP at a rate of 49 ± 8 nm/s. These results indicate that the inhibition of motility observed with Tm-2 ceased when native loop 4 of Myo1b was truncated.

Myo1b-GAGEGA also supported the translocation of actin (38 ± 6 nm/s). Myo1b-GAGEGA translocated Tm-2−actin filaments at a rate comparable to that of actin only (41 ± 5 nm/s), indicating that replacing endogenous loop 4 of Myo1b with the shorter loop 4 from *Dictyostelium* myosin II also relieved the inhibition of Tm-2 on Myo1b.

Both mutants appeared to translocate actin filaments at rates greater than that of the wild type. At comparable protein concentrations, Myo1b-NGLD translocated actin at 34 ± 9 vs 20 ± 5 nm/s for Myo1b-WT, suggesting that substituting loop 4 significantly affected the speed. The rate of translocation by Myo1b-GAGEGA was also faster than that determined for Myo1b-WT (38 ± 6 nm/s for Myo1b-NGLD vs 20 ± 5 nm/s for Myo1b-WT) with the caveat that in this case the Myo1b concentrations were not equivalent, which might partially account for the difference.

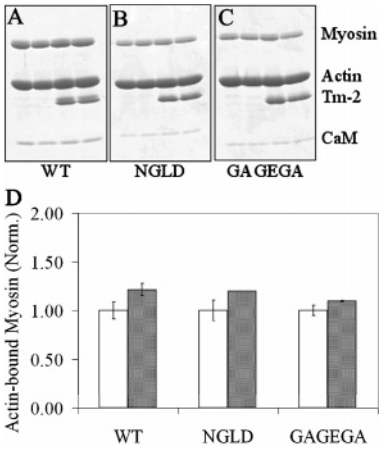

FIGURE 5: Cosedimentation assays of Myo1b^{1IQ} and loop 4 mutants in the presence and absence of Tm-2. Duplicate samples of Myo1b^{1IQ} (A) and loop 4 mutants, Myo1b^{1IQ}-NGLD (B) and Myo1b^{1IQ}-GAGEGA (C) (~7 μg), were incubated with 6 μM filamentous actin in the absence (lanes 1 and 2) or presence (lanes 3 and 4) of 2.5 μM Tm-2 in 10 mM Tris (pH 7.5), 50 mM KCl, 1 mM $MgCl_2$, 1 mM DTT, and 2 mM CaEGTA (pCa 4.6). Shown are the amounts of actin, Tm-2, myosin I, and calmodulin (CaM) found in the pellets. The myosin I associated with the pellets was quantified with NIH Image and normalized for both Myo1b^{1IQ}-WT and loop 4 mutants (D): (white) without Tm-2 and (gray) with Tm-2.

Table 3: Myo1b-Mediated Movement of Actin in the Presence and Absence of Tropomyosin-2[a]

	without Tm-2 (nm/s)	with Tm-2 (nm/s)
Myo1b-WT	20 ± 5 (145)	small fraction of motile filaments; most actin is loosely attached to substrate
Myo1b-NGLD	34 ± 9 (35)	49 ± 8 (39)
Myo1b-GAGEGA	38 ± 6 (180)	41 ± 5 (180)

[a] Average speed ± the standard deviation (number of filaments).

Cellular Localization of Myo1b and Loop 4 Mutants. Full-length myc-tagged Myo1b was expressed in HeLa (cervical cancer epithelial) cells, and its localization was determined after 18 h by indirect immunomicroscopy (Figure 6). As previously observed, expressed Myo1b appeared at the cell membrane and in punctae throughout the cytoplasm (Figure 6B) (*4*, *35*). In some regions, Myo1b appeared to be filamentous in nature. Electron microscopy studies have previously shown Myo1b in association with actin filaments (*36*). Myo1b was, however, not found to colocalize with actin filaments assembled into stress fibers as identified by the presence of tropomyosin (Figure 6A) or with bundles of actin filaments visualized with rhodamine phalloidin (data not shown). In addition, no difference in the localization of Myo1b-EGFP from that of myc-tagged Myo1b was observed; moreover, the same results were obtained with NRK cells (data not shown).

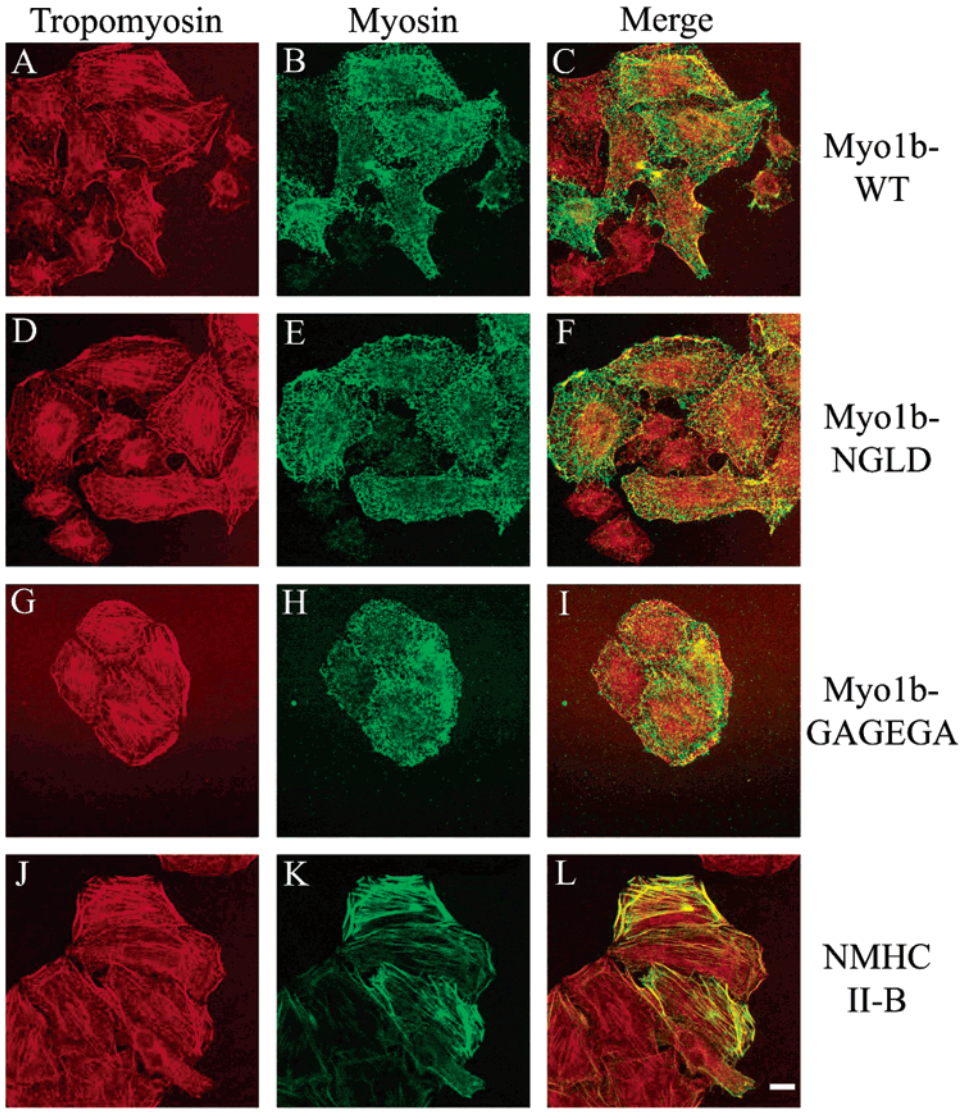

FIGURE 6: Localization of expressed wild-type Myo1b and loop 4 mutants in HeLa cells. Cells were transiently transfected for 18 h, fixed and permeabilized with cytoskeleton stabilization buffer containing streptolysin-O, and then stained for tropomyosin with mouse monoclonal anti-TM followed by goat anti-mouse IgG-Alexa^{568} (A, D, and G) and rabbit polyclonal anti-myc followed by goat anti-rabbit IgG-Alexa^{488} to visualize Myo1b (B, E, and H) before being viewed by confocal microscopy. Merged images are shown in panels C, F, and I. Control cells expressing GFP-tagged non-muscle myosin II-B are shown in panels J−L. Unlike Myo1b or Myo1b loop 4 mutants, non-muscle myosin II-B colocalized with tropomyosin-containing filaments as shown in the merged image in panel L. The scale bar is 10 μm.

Similarly, by indirect immunofluorescence microscopy with anti-myc, the appearance of expressed Myo1b-NGLD (Figure 6E) and Myo1b-GAGEGA (Figure 6H) in the cells appeared largely punctate or in some cases filamentous as seen for Myo1b-WT. As observed with Myo1b-WT, neither Myo1b-NGLD nor Myo1b-GAGEGA colocalized with tropomyosin-containing stress fibers (Figure 6F,I). On the other hand, enhanced GFP-tagged non-muscle myosin II-B associated with tropomyosin-containing stress fibers (Figure 6J−L), as previously observed (*31*).

DISCUSSION

The studies described here show that truncation of loop 4 in Myo1b from RMNGLDES to NGLD, and substitution of wild-type loop 4 in Myo1b with the loop 4 sequence from *Dictyostelium* myosin II, GAGEGA, reverse the inhibition of the actin-activated Mg^{2+}-ATPase activity of Myo1b seen in the presence of Tm-2. The experiments were repeated with fibroblast tropomyosin 5a (*37*) with similar results (data not shown), indicating that the tropomyosin isoform is not critical.

The studies demonstrate the involvement of loop 4, a structural element in the upper 50 kDa subdomain of the Myo1b motor domain, in mediating the interaction of Myo1b with actin-tropomyosin. The mutant loops used in the study both contain a single negatively charged amino acid and do not result in an overall net change in the charge of the loop from the wild type, suggesting that the difference in the actin-activated Mg^{2+}-ATPase activity and motility of wild-type Myo1b versus the loop 4 mutants in the presence of tropomyosin is due to the shorter length of the mutant loops.

The studies are consistent with analysis of the crystal structure of MyoE, a related myosin I, which showed that the extended loop 4 of class I myosins, which is located at the actin-binding site, could interfere with the interaction of myosin I with actin when actin-binding proteins such as tropomyosin, which bind along the length of the actin filament, are present (*12*). Our cosedimentation studies do

not show that loop 4 prevents binding of Myo1b to actin-tropomyosin. Instead, our studies indicate that Myo1b binds to actin-tropomyosin while inhibiting the actin-activated ATPase activity, suggesting that a kinetic step when Myo1b is bound to actin is being affected. The actin-activated ATPase activity of myosin II has previously been shown to be inhibited by troponin−tropomyosin complexes without any effect on myosin binding (*38*). A conformational change in myosins accompanying phosphate release might be prevented in the presence of tropomyosin (*38*).

One discrepancy in our results is that the cosedimentation assays show that $Myo1b^{1IQ}$ and the loop 4 mutants all bind filamentous actin to the same extent with or without Tm-2; however, in motility assays, there was a clear distinction in the number of actin filaments that bound to Myo1b with or without Tm-2, with only a small percentage of actin−tropomyosin filaments attaching (loosely) to immobilized Myo1b. This may be due to the difference in flexibility of immobilized Myo1b versus Myo1b in solution.

Lehman and colleagues have shown that tropomyosins can bind to the inner or outer domain of actin depending on the particular actin or tropomyosin isoform (*39*). Skeletal muscle tropomyosin and fibroblast tropomyosin 5a both bind to the inner domain of actin (*39*). Structural studies of Myo1b are limited. Studies of Myo1b with actin-tropomyosin would reveal the relationship among the three proteins.

Our results showed that modifying loop 4, which is not near the nucleotide-binding region, increased the rate at which Myo1b translocates actin in vitro. Studies with Myo1b and other myosins have shown that surface loops have considerable influence on myosin kinetics. Modifying loop 1, a surface loop that lies between the nucleotide-binding regions and switch I of Myo1b, affects actin affinity, ATPase activity, and nucleotide access (*40*).

The increase in the rate of translocation by Myo1b-NGLD and Myo1b-GAGEGA over that of wild-type Myo1b might be ascribed to a reduction in steric hindrance due to the shorter loop 4 forms, or deletion of the charged amino acids arginine and glutamic acid. The results cannot, however, be attributed to a change in the net charge of loop 4 unlike the previous studies with smooth muscle myosin II, which showed that mutagenesis of the C-loop involving a single charge change altered the actin-activated ATPase activity and in vitro motility (*16*).

Although the in vitro studies support the contention that the presence of tropomyosin affects Myo1b's ability to hydrolyze ATP and translocate actin, our results also indicate that loop 4 does not singly determine whether Myo1b associates with tropomyosin-containing stress fibers in cells. When expressed in tissue culture cells, tagged Myo1b in which loop 4 is truncated or replaced with a shorter loop from another myosin does not associate with stress fibers. These same results were observed in two different cell lines, indicating that the results were not cell-specific. In addition, the same results were observed over a range of fixation conditions and transfection conditions, resulting in different expression levels of Myo1b.

Unlike the actin in protrusions such as lamellipodia and filopodia, which are considered to be highly dynamic structures (*4*, *35*), stress fibers are comparatively stable due to the presence of other actin-binding proteins, including, but not limited to, tropomyosins. Other actin-binding proteins, including α-actinin, caldesmon, and filamin, are also found in association with stress fibers. It is reasonable to postulate that these proteins and/or others found on stress fibers compete for similar sites on actin as Myo1b, thereby contributing to the exclusion of Myo1b from stress fibers.

These results contribute to what is known regarding targeting of molecular motors in the cell. Previous studies have indicated that the tail region of Myo1b contains information required for intracellular targeting, although binding is enhanced by a component of the motor domain (*35*). Although the tail region might dictate the subcellular membranes with which Myo1b associates, specific structural elements in the motor domain, including loop 4, might prevent the association of Myo1b with certain subpopulations of actin filaments in the cell.

ACKNOWLEDGMENT

We thank Dr. Steen H. Hansen (Children's Hospital, Boston, MA) for help with design of the constructs, Dr. Michael Geeves (University of Kent, Canterbury, U.K.) for helpful discussion, and Dr. David Helfman (University of Miami, Coral Gables, FL) for the Tm-2 clone.

REFERENCES

1. Mooseker, M. S., and Cheney, R. E. (1995) Unconventional myosins, *Annu. Rev. Cell Dev. Biol. 11*, 633−675.
2. Berg, J. S., Powell, B. C., and Cheney, R. E. (2001) A millennial myosin census, *Mol. Biol. Cell 12*, 780−794.
3. Foth, B. J., Goedecke, M. C., and Soldati, D. (2006) New insights into myosin evolution and classification, *Proc. Natl. Acad. Sci. U.S.A. 103*, 3681−3686.
4. Tang, N., and Ostap, E. M. (2001) Motor domain-dependent localization of myo1b (myr-1), *Curr. Biol. 11*, 1131−1135.
5. Gunning, P. W., Schevroz, G., Kee, A. J., and Hardeman, E. C. (2005) Tropomyosin isoforms: Divining rods for actin cytoskeleton function, *Trends Cell Biol. 15*, 333−341.
6. Bernstein, B. W., and Bamburg, J. R. (1982) Tropomyosin binding to F-actin protects the F-actin from disassembly by brain actin-depolymerizing factor (ADF), *Cell Motil. 2*, 1−8.
7. Fattoum, A., Hartwig, J. H., and Stossel, T. P. (1983) Isolation and some structual and functional properties of macrophage tropomyosin, *Biochemistry 22*, 1187−1193.
8. Ishikawa, R., Yamashiro, S., and Matsumura, F. (1989) Differential modulation of actin-severing activity by multiple isoforms of cultured rat cell tropomyosin, *J. Biol. Chem. 264*, 7490−7497.
9. Blanchoin, L., Pollard, T. D., and Hitchcock-DeGregori, S. E. (2001) Inhibition of the Arp2/3 complex-nucleated actin polymerization and branch formation by tropomyosin, *Curr. Biol. 11*, 1300−1304.
10. Perry, S. V. (2001) Vertebrate tropomyosin: Distribution, properties and function, *J. Muscle Res. Cell Motil. 22*, 5−49.
11. Milligan, R. A. (1996) Protein-protein interactions in the rigor actomyosin complex, *Proc. Natl. Acad. Sci. U.S.A. 93*, 21−26.
12. Kollmar, M., Durrwang, U., Kliche, W., Manstein, D. J., and Kull, F. J. (2002) Crystal structure of the motor domain of a class-I myosin, *EMBO J. 21*, 2517−2525.
13. Ajtai, K., Garamszegi, S. P., Park, S., Velazquez Dones, A. L., and Burghardt, T. P. (2001) Structural characterization of β-cardiac myosin subfragment 1 in solution, *Biochemistry 40*, 12078−12093.
14. Rayment, I., Holden, H. M., Whittaker, M., Yohn, C. B., Lorenz, M., Holmes, K. C., and Milligan, R. A. (1993) Structure of the actin-myosin complex and its implications for muscle contraction, *Science 261*, 58−65.
15. Liu, Y., Scolari, M., Im, W., and Woo, H.-J. (2006) Protein-protein interactions in actin-myosin binding and structural effects of R405Q mutation: A molecular dynamics study, *Proteins: Struct., Funct., Bioinf. 64*, 156−166.
16. Ajtai, K., Garamszegi, S. P., Watanabe, S., Ikebe, M., and Burghardt, T. P. (2004) The myosin cardiac loop participates functionally in the actomyosin interaction, *J. Biol. Chem. 279*, 23415−23421.

17. Spudich, J. A., and Watt, S. (1971) The regulation of rabbit skeletal muscle contraction. I. Biochemical studies of the interaction of the tropomyosin-troponin complex with actin and the proteolytic fragments of myosin, *J. Biol. Chem. 246*, 4866−4871.
18. MacLean-Fletcher, S., and Pollard, T. D. (1980) Identification of a factor in conventional muscle actin preparations which inhibits actin filament self-association, *Biochem. Biophys. Res. Commun. 96*, 18−27.
19. Maytum, R., Konrad, M., Lehrer, S. S., and Geeves, M. A. (2001) Regulatory properties of tropomyosin effects of length, isoform, and N-terminal sequence, *Biochemistry 40*, 7334−7341.
20. Kabsch, W., and Sander, C. (1983) Dictionary of protein secondary structure: Pattern recognition of hydrogen-bonded and geometrical features, *Biopolymers 22*, 2577−2637.
21. Fisher, A. J., Smith, C. A., Thoden, J., Smith, R., Sutoh, K., Holden, H. M., and Rayment, I. (1995) Structural studies of myosin:nucleotide complexes: A revised model for the molecular basis of muscle contraction, *Biophys. J. 68*, 19S−28S.
22. Perreault-Micale, C., Shushan, A. D., and Coluccio, L. M. (2000) Truncation of a mammalian myosin I results in loss of Ca^{2+}-sensitive motility, *J. Biol. Chem. 275*, 21618−21623.
23. Geeves, M. A., Perreault-Micale, C., and Coluccio, L. M. (2000) Kinetic analyses of a truncated mammalian myosin I suggest a novel isomerization event preceding nucleotide binding, *J. Biol. Chem. 275*, 21624−21630.
24. Ashley, C. C., and Moisescu, D. G. (1977) Effect of changing the composition of the bathing solutions upon the isometric tension-pCa relationship in bundles of crustacean myofibrils, *J. Physiol. (Oxford, U.K.) 270*, 627−652.
25. Moisescu, D. G., and Thieleczek, R. (1978) Calcium and strontium concentration changes within skinned muscle preparations following a change in the external bathing solution, *J. Physiol. (Oxford, U.K.) 275*, 241−262.
26. Pollard, T. D. (1982) Myosin purification and characterization, *Methods Cell Biol. 24*, 333−371.
27. Coluccio, L. M., and Bretscher, A. (1987) Calcium-regulated cooperative binding of the microvillar 110K-calmodulin complex to F-actin: Formation of decorated filaments, *J. Cell Biol. 105*, 325−333.
28. Laemmli, U. K. (1970) Cleavage of structural proteins during the assembly of the head of bacteriophage T4, *Nature 227*, 680−685.
29. Toyoshima, Y. Y., Kron, S. J., McNally, E. M., Niebling, K. R., Toyoshima, C., and Spudich, J. A. (1987) Myosin subfragment-1 is sufficient to move actin filaments in vitro, *Nature 328*, 536−539.
30. Williams, R., and Coluccio, L. M. (1994) Novel 130-kDa rat liver myosin-1 will translocate actin filaments, *Cell Motil. Cytoskeleton 27*, 41−48.
31. Wei, Q., and Adelstein, R. S. (2000) Conditional expression of a truncated fragment of nonmuscle myosin II-A alters cell shape but not cytokinesis in HeLa cells, *Mol. Biol. Cell 11*, 3617−3627.
32. Coluccio, L. M., and Geeves, M. A. (1999) Transient kinetic analysis of the 130-kDa myosin I (myr 1 gene product) from rat liver: A myosin I designed for maintenance of tension? *J. Biol. Chem. 274*, 21575−21580.
33. Zhu, T., Sata, M., and Ikebe, M. (1996) Functional expression of mammalian myosin Iβ: Analysis of its motor activity, *Biochemistry 35*, 513−522.
34. Zhu, T., Beckingham, K., and Ikebe, M. (1998) High affinity Ca^{2+} binding sites of calmodulin are critical for the regulation of myosin Iβ motor function, *J. Biol. Chem. 273*, 20481−20486.
35. Ruppert, C., Godel, J., Müller, R. T., Kroschewski, R., Reinhard, J., and Bähler, M. (1995) Localization of the rat myosin I molecules myr 1 and myr 2 and in vivo targeting of their tail domains, *J. Cell Sci. 108*, 3775−3786.
36. Raposo, G., Cordonnier, M. N., Tenza, D., Menichi, B., Durrbach, A., Louvard, D., and Coudrier, E. (1999) Association of myosin I α with endosomes and lysosomes in mammalian cells, *Mol. Biol. Cell 10*, 1477−1494.
37. Pittenger, M. F., Kazzaz, J. A., and Helfman, D. M. (1994) Functional properties of non-muscle tropomyosin isoforms, *Curr. Opin. Cell Biol. 6*, 96−104.
38. Chalovich, J. M., and Eisenberg, E. (1982) Inhibition of actomyosin ATPase activity by troponin-tropomyosin without blocking the binding of myosin to actin, *J. Biol. Chem. 257*, 2432−2437.
39. Lehman, W., Hatch, V., Korman, V., Rosol, M., Thomas, L., Maytum, R., Geeves, M. A., Van Eyk, J. E., Tobacman, L. S., and Craig, R. (2000) Tropomyosin and actin isoforms modulate the localization of tropomyosin strands on actin filaments, *J. Mol. Biol. 302*, 593−606.
40. Clark, R., Ansari, M. A., Dash, S., Geeves, M. A., and Coluccio, L. M. (2005) Loop 1 of transducer region in mammalian class I myosin, Myo1b, modulates actin affinity, ATPase activity, and nucleotide access, *J. Biol. Chem. 280*, 30935−30942.

BI602439F